

Nutritional Evaluation of Beetroot Dried using Novel Thermal Storage-based Passive Solar Dryers

Ankit Kumar^{1*}, D K Vyas² and Sravankumar Jogunuri³

ABSTRACT

This study investigates the thermal performance and drying efficiency of an indirect passive solar dryer (IPSD) integrated with three thermal energy storage (TES) materials-river pebbles, grit, and recycled metal bottle caps-for dehydration of beetroot (*Beta vulgaris*) slices of 2, 4, and 6 mm thickness under semi-arid climatic conditions in Gujarat, India. The IPSD consisted of a 1.5 m² blackened aluminium absorber plate covered with 4 mm toughened glass glazing and inclined at 25°. TES materials were arranged in a 3 cm thick bed, exhibiting thermal conductivities of 0.22 W m⁻¹ K⁻¹ (pebbles), 1.5 W m⁻¹ K⁻¹ (grit), and 160 W m⁻¹ K⁻¹ (metal bottle caps). Thermal analysis revealed that the metal bottle cap configuration achieved the best overall performance, attaining a peak heat recovery ratio of 161.24% during the discharging phase and the highest average charging-phase thermal efficiency of 59.70%, outperforming grit (36.32%) and pebbles (42.26%). Although grit recorded the highest peak collector temperature (112 °C), metal bottle caps sustained the greatest rise in outlet air temperature (up to 45 °C above ambient), ensuring stable drying conditions. Drying experiments showed that metal bottle caps reduced moisture content to 5.59% for 2 mm slices in the shortest drying duration while minimising nutrient losses. Proximate analysis indicated enhanced retention of protein (10.17%), ascorbic acid (10.23 mg/100 g), and total phenolics (128 mg/100 g) compared to open sun drying. A 4 mm slice thickness provided an optimal balance between drying rate and quality retention. The study establishes recycled metal bottle caps as an efficient, low-cost, and sustainable TES material for passive solar drying applications.

Keywords: Beetroot drying, Drying kinetics, Indirect passive solar dryer, Solar dryers, Thermal energy storage

ARTICLE INFO

Received on	:	19/01/2026
Accepted on	:	14/02/2026
Published online	:	31/03/2026



INTRODUCTION

Solar drying is a transformative technology for reducing post-harvest food losses, particularly in regions where losses can reach 30-40% due to inadequate preservation methods (Matavel et al., 2022). By harnessing renewable solar energy, solar dryers provide a sustainable alternative to conventional methods, enhancing food quality and reducing greenhouse gas emissions (Rulazi et al., 2023). These systems are broadly categorised into passive and active types, with further subdivisions into direct, indirect, and mixed-mode designs (Ekechukwu and Norton, 1997a). Passive systems, particularly single-glazed flat-plate collectors, offer an efficient and economical solution for rural uses because they rely on natural convection (Ekechukwu and Norton, 1997b). Kapadiya and Desai (2014) emphasised that solar systems are a sustainable method for preserving food quality while significantly reducing fossil fuel usage. Gupta et al. (2017) developed a passive dryer using local material that achieved effective drying temperatures in the range of 35–65°C. Kumar et al. (2015) utilised a cabinet-type solar dryer integrated with an Artificial Neural Network (ANN) prediction for biomass drying, reporting high thermal and exergy efficiencies. Fernandes and Tavares (2024) provided comprehensive

classifications of solar dryers, promoting hybrid systems integrated with thermal energy storage (TES) and Photovoltaics (PV) for continuous, and eco-friendly operation.

However, the intermittency of solar radiation necessitates the use of TES materials to ensure operational continuity. Bala and Woods (1994) pioneered the use of river stones in solar dryers to improve heat retention and consistency of drying. Boukar et al. (2024) analysed pozzolan stones and identified that specific sizes and configurations are required for maximum thermal performance. Kalidasan et al. (2020) highlighted the integration of Phase Change Materials (PCMs), such as paraffin and stearic acid, to enhance conductivity and thermal reliability. Koçak et al. (2020) reviewed sensible thermal energy storage (STES) using materials like basalt and NaCl, citing efficiencies exceeding 90%. Deepak and Behura (2025) demonstrated a system that combines pebbles and PCM, halving the drying time and improving exergy efficiency. Furthermore, Allouhi (2023) confirmed the feasibility of large-scale latent thermal energy storage (LTES) systems using adipic acid for industrial solar drying.

¹B.Tech Agricultural Engineering, Dept. of Renewable Energy Engineering, College of Agricultural Engineering and Technology, Anand Agricultural University, Godhra, India

²Professor & Head, 3 Assistant Professor, Dept. of Renewable Energy Engineering, College of Agricultural Engineering and Technology, Anand Agricultural University, Godhra, India

^{*}Corresponding Author E-mail: ankitoday123@gmail.com

In the specific context of beetroot drying, these thermal technologies address unique challenges regarding temperature control and efficiency. Fudholi et al. (2010) reviewed over 25 types of solar dryers, noting that they can achieve internal temperatures of up to 85°C with efficiencies ranging from 17% to 70%. Onuigbo et al. (2017) developed a dryer that achieved rapid drying rates and quality preservation. Anand Inamdar et al. (2021) successfully used PCM to prolong the process post-sunset. Ankush (2024) achieved a moisture content drop from 611% to 6% (db) in 33 hours, resulting in enhanced colour and sugar content. Mehta et al. (2025) further demonstrated that PCM-integrated dryers can effectively maintain drying temperatures after peak solar hours, confirming that dryer design and heat storage significantly impact efficiency.

The drying method also dictates the nutritional profile of the final beetroot product. Bhavani et al. (2022) found solar drying superior to other methods, preserving 2.78 g of fibre, 8.06% ash, and 93.52% dry matter. Singh et al. (2024) confirmed beetroot's rich nutritional profile and its successful application in fortified foods. Moreover, studies by Ojeniran et al. (2025) have demonstrated that solar drying at moderate temperatures best retains macronutrients and bioactives, such as betalains and ascorbic acid, whereas tray and open-sun drying often result in greater nutrient losses. Distinct from previous studies that relied on low-conductivity natural stones or economically prohibitive phase change materials, while this research presents the thermal and nutritional evaluation of discarded metal bottle caps as a sensible heat storage medium. Unlike mild steel chips or crushed cans, which often require significant processing, metal bottle caps offer a unique, ready-to-use geometry with high thermal conductivity and optimal void fraction for air turbulence. This study aims to bridge the gap between waste valorisation and food security by demonstrating how a zero-cost municipal waste product can outperform traditional storage materials in preserving the bioactive compounds of beetroot.

MATERIALS AND METHODS

Study Area and Climatic Conditions

The present study was conducted at the Department of Renewable Energy Engineering, Anand Agricultural University, Godhra, Gujarat, India (22.7757° N, 73.6145° E; elevation 111 meters above MSL). The region experiences a semi-arid climate with high solar insolation (5.5-6.2 kWh/m²/day) and ambient temperatures ranging from 21°C to 39°C during the experimental period, offering optimal conditions for solar drying applications.

Table 1: Environmental conditions during the experiment

Test Configuration	Avg. Ambient Temp (°C)	Max. Solar Radiation (W/m ²)	Avg. Wind Speed (m/s)
No Load (Control)	26.8	446	0.5-1.8
Pebbles	29.22	402	0.5-2
Grit	32.46	460	0.5-1.8
Metal bottle caps	30.13	494	0.5-2.5

Experiments were conducted during the dry season (December-April), ensuring consistent solar radiation, low humidity, and stable ambient temperatures. Solar irradiance ranged between 150 and 450 W/m², with an average exceeding 270 W/m². Wind speeds varied moderately (0.5-2.5 m/s), aligning with the passive ventilation design. This climatic consistency across experimental days ensured that the observed thermal variations stemmed predominantly from the TES material rather than environmental anomalies.

Experimental Design

The experimental framework of this study was systematically divided into four distinct phases. Initially, the thermal evaluation of an IPSD integrated with various TES materials was conducted to determine optimal configurations. This was followed by a comprehensive assessment of the drying performance of beetroot slices using three comparative systems: the modified IPSD, a cabinet solar dryer, and open sun drying. The third phase focused on the proximate and nutritional composition analysis of the dried beetroot to evaluate the retention of quality. Finally, a comparative performance and quality analysis was conducted to examine trends across the different drying systems and slice thicknesses.

Dryer Description and TES Material Integration
Indirect passive solar dryer



Fig. 1: Indirect passive solar dryer

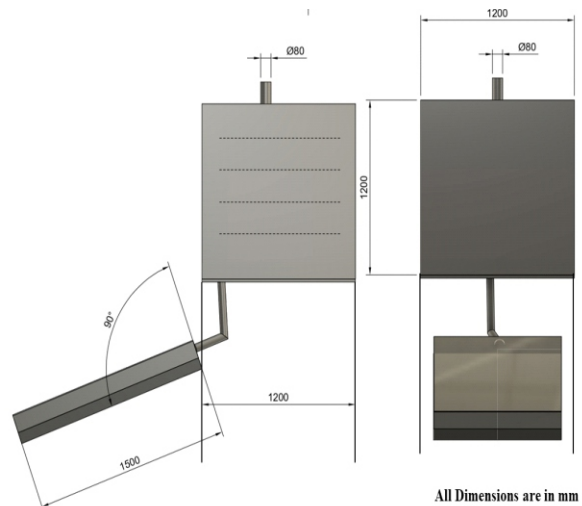


Fig. 2: Schematic view of the indirect passive solar dryer with dimensional specifications (all units in mm)

The experimental setup consisted of a custom-designed indirect passive solar dryer (IPSD) comprising a solar air heater, an insulated air duct, and a drying chamber (Fig. 1). The solar air heater utilised a flat-plate collector with practical dimensions of 1.5 m × 1.0 m, resulting in a total collector area of 1.5 m². The absorber plate was fabricated from black-painted aluminium, insulated with 5 cm thick glass wool to minimise thermal losses, and covered with 4 mm thick toughened glass glazing. The collector was oriented southward with a tilt angle of 25°, optimised for maximum solar insolation.

Heated air from the collector was channelled through an insulated duct into the drying chamber, which was constructed using double-layer polycarbonate sheets with internal dimensions of 1.5 m × 1.5 m × 1.5 m. To ensure continuous natural convection via the stack effect, multiple circular air outlets (50 mm diameter) were strategically positioned at the top of the drying chamber, facilitating effective moisture removal during the drying process.

TES materials and configurations



Fig. 3: Different types of TES-based solar drying systems

To evaluate thermal performance, the solar collector was tested under four distinct configurations. The control setup (No TES) operated with an empty absorber plate, utilising only air as the heat transfer medium. The three experimental configurations involved integrating specific thermal energy storage (TES) materials: rounded river stones (pebbles) with a diameter of 2-3 cm, painted black to enhance solar absorption; crushed grit (1-2 cm), selected for its high density and specific heat capacity; and black-painted metal bottle caps reused from beverage containers, which served as novel, low-cost, and high-conductivity TES material.

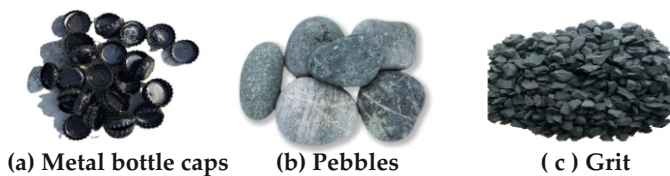


Fig. 4: Thermal Energy Storage (TES) materials used in the study: (a) Metal bottle caps, (b) Pebbles, and (c) Grit

Table 2: Thermal property of thermal energy storage material

Property	Aluminium Metal bottle caps	River Bed Pebble (Bulk Bed)	Grit (Gritstone)
Thermal Conductivity	~160 W/m·K	0.22 W/m·K (Wada et al., 2024)	~1.5 W/m·K (Robertson, 1988)
Thermal Diffusivity	~62 mm ² /s	0.15 mm ² /s (Wada et al., 2024)	~0.5-1.5 mm ² /s (Robertson, 1988)
Specific Heat Capacity	~900 J/kg·K	~800 J/kg·K (Robertson, 1988)	~740-800 J/kg·K (Wada et al., 2024)
Density	2,700 kg/m ³	~2,600 kg/m ³ (Robertson, 1988; Wada et al., 2024)	~2,200-2,600 kg/m ³ (Robertson, 1988)
Porosity	N/A	33.31% (Wada et al., 2024)	~20-35%

Each material was uniformly spread over the absorber plate to a depth of 3 cm.

Measurement of Thermal Performance

The experimental system was operated daily between 08:30 and 18:10 under clear-sky conditions. To capture dynamic thermal performance, key parameters were recorded at 10-minute intervals. Solar irradiance was measured using a pyranometer (Apogee SP-215), while ambient temperature and relative humidity were monitored with a digital hygrometer. K-type thermocouples connected to a 12-channel digital data logger (HTC™) were employed to record inlet and outlet air temperatures. Furthermore, the surface temperature of the TES material was assessed using a laser infrared thermometer. Air velocity within the system was measured using a digital vane anemometer, and external wind conditions (speed and direction) were tracked using a cup anemometer and wind vane.

Thermal calculations

Mass flow rate of air (ṁ):

The mass flow rate of air through the solar collector was calculated using the continuity equation, which relates air density, velocity, and the cross-sectional area of the collector duct (Duffie & Beckman, 2013). This parameter quantifies the volume of air available for heat transfer and moisture removal during the drying process

$$\dot{m} = \rho \cdot V \cdot A_{coll}$$

Where, ṁ is the mass flow rate of air (kg/s), ρ is the density of air, and V is the velocity of air and A_{coll} = Area of collector

• **Useful heat gain (Q_u):**

The useful heat gain represents the net thermal energy absorbed by the air stream as it passes through the solar collector, determined from the temperature difference between inlet and outlet air (Duffie & Beckman, 2013). This metric is fundamental for evaluating the energy-

conversion performance of the flat-plate collector across varying TES configurations.

$$Q_u = \dot{m} * C_p * (T_o - T_i)$$

Where, \dot{m} is the mass flow rate of air (kg/s), C_p is the specific heat capacity of air at the given temperature (kJ/kg K) and T_o , T_i are the Outlet and Inlet Temperature of the collector, respectively

- **Thermal efficiency (η):**

Thermal efficiency is defined as the ratio of useful heat gain to the total solar energy incident on the collector surface, expressed as a percentage (Ekechukwu and Norton, 1997a). It provides a standardised measure of the collector's effectiveness in converting incoming solar radiation into usable thermal energy for drying.

$$\eta_{th} = \frac{Q_u}{I_t A_c}$$

Where, η_{th} =thermal efficiency, Q_u =Useful energy, I_t =Irradiance (W/m^2) and A_c =Collector area

- **Heat recovery ratio (HRR)**

The heat recovery ratio quantifies the proportion of stored thermal energy that is released by the TES material during the discharging phase relative to the instantaneous solar energy input (Koçak et al., 2020). Values exceeding 100% indicate that the thermal energy released from storage surpasses the concurrent solar input, confirming effective heat buffering during periods of declining irradiance.

$$HRR = \frac{Q_U}{I_t * A_c} * 100$$

Hourly and average efficiencies were calculated for each TES setup to assess its dynamic thermal behaviour.

Drying Trials of Beetroot

Sample preparation

Fresh, mature beetroots were sourced from local farms. After washing and peeling, the roots were sliced into three thicknesses: 2 mm (T2), 4mm (T4), and 6 mm (T6) using vegetable slicer. Each batch consisted of 100 g of uniformly sized slices, which were blotted to remove surface moisture before drying.

Drying systems evaluated for beetroot drying



Fig. 5: Different Systems used for Beetroot Drying

- **Modified IPSD with metal bottle caps TES (D)**

This indirect system was designed to prioritise product quality by preventing direct solar exposure. Ambient air was preheated as it passed over the high-conductivity metal bottle cap bed in the collector, then rose into the drying chamber via the stack effect. The bottle caps served as a thermal buffer, stabilising air temperatures and mitigating fluctuations caused by intermittent cloud cover.

- **Cabinet solar dryer (c)**

Functioning as a direct mixed-mode system, this dryer utilised an insulated box to trap solar energy. The resulting greenhouse effect heated the beetroot slices simultaneously through convection and direct radiation. While this method achieved higher peak temperatures, the lack of thermal storage reduced thermal inertia and increased sensitivity to environmental changes.

- **Open sun drying (O)**

Serving as the experimental control, this method involved spreading beetroot slices on elevated stainless-steel trays covered with nylon mesh to prevent contamination. Relying solely on ambient solar irradiance and natural wind currents, the process exhibited slower, more variable drying rates, providing a baseline for quantifying the efficiency gains of the engineered dryers.

Drying was carried out from 9:00 AM to 5:00 PM until the sample reached a constant weight. Hourly weights were recorded using a digital balance (± 0.01 g).

Drying rate and moisture loss

To evaluate the drying kinetics, the moisture removal behaviour of the beetroot slices was monitored at hourly intervals. The moisture content (MC) was calculated on a dry basis to provide a consistent standard for comparison across different drying times. Subsequently, the drying rate (DR) was determined as the quantity of moisture evaporated per unit of dry matter per hour. These parameters were calculated using the recorded weight changes of the samples until a constant equilibrium weight was achieved, using the following equations:

- **Moisture content (% dry basis):**

$$MC_t(db) = \frac{W_t - W_d}{W_d}$$

- **Drying rate (g water/g dry matter/h):**

$$DR = \frac{MC_t - MC_{t+1}}{T_{t+1} - T_t}$$

Where MC is the moisture content (% db), W_t is the weight of the sample at time t (g), W_d is the weight of dry matter (g), DR is the drying rate (g water/g dry matter/h), and T is the time interval (h), respectively.

Proximate and Nutritional Analysis

Proximate composition analysis was carried out to assess the

nutritional integrity and quality of beetroot slices dried using three different methods-modified indirect passive solar dryer (IPSD), cabinet dryer, and open sun drying-across three slice thicknesses (2 mm, 4 mm, and 6 mm). The analyses were performed in the post-harvest laboratory of the Department of Food Processing Technology, Anand Agricultural University, following the standardised guidelines of the Food Safety and Standards Authority of India (FSSAI, 2016).

Proximate composition

The proximate composition of the dried beetroot slices was analysed in triplicate following standard protocols. Moisture content was determined using the hot air oven method at 105±2°C until a constant weight was achieved, while crude protein content was estimated using the Kjeldahl nitrogen analysis method (N × 6.25) to quantify thermal degradation (AOAC, 2005). Crude fat was extracted using petroleum ether in a Soxhlet apparatus for 6 hours, and crude fibre was estimated via the acid-alkali digestion method involving sequential boiling in dilute sulfuric acid and sodium hydroxide (Ranganna, 1986). Total ash content was determined by incinerating samples in a muffle furnace at 550°C for 3 hours to measure mineral retention, and total carbohydrates were calculated by difference (subtracting moisture, protein, fat, ash, and fibre from 100) to estimate the energy value.

Bioactive and physicochemical properties

To evaluate the retention of bioactive compounds and physical quality, specific biochemical markers were assessed. Ascorbic acid (Vitamin C) was measured using the 2,6-dichlorophenolindophenol (DCPIP) titrimetric method, while total phenolic content was quantified using the Folin-Ciocalteu colourimetric method at 765 nm, expressed as mg gallic acid equivalent (GAE)/100 g (Malik & Singh, 1980). Betalain pigments (betacyanin and betaxanthin) were extracted with 80% methanol and determined spectrophotometrically at 538 nm and 480 nm, respectively (Shakir & Simone, 2024). Titratable acidity (TTA) was determined by titrating aqueous extracts with 0.1 N NaOH and expressed as per cent citric acid. Finally, colour parameters were evaluated using a portable digital colourimeter based on the CIELAB system, where L* indicates lightness (0 = black, 100 = white), a* represents the red-green chromaticity, and b* denotes the yellow-blue chromaticity. This detailed colour profiling helped quantify pigment degradation and visual appeal across the different drying conditions and slice thicknesses

RESULTS AND DISCUSSION

This section presents the thermal performance, drying kinetics, and nutritional quality of beetroot dried using an indirect passive solar dryer (IPSD) integrated with various thermal energy storage (TES) materials. Three drying systems were compared: the modified IPSD with metal bottle caps, a cabinet solar dryer, and open sun drying. Key performance indicators included temperature gradients, collector efficiency, drying rates, and nutritional composition across three slice thicknesses (2 mm, 4 mm, and 6 mm).

Thermal Performance of Indirect Passive Solar Dryer

The thermal evaluation of the indirect passive solar dryer forms the backbone of this investigation, as it underpins the efficacy of low-energy drying methods in preserving agricultural quality. The thermal performance of the system was quantitatively evaluated using time-resolved temperature and efficiency metrics under four configurations: without TES (control), and with pebbles, grit, and black-painted metal bottle caps as thermal energy storage (TES) media. Each configuration was evaluated in terms of environmental consistency, internal temperature distribution, heat retention, collector outlet temperature, and thermal efficiency.

Thermal profiling and heat distribution

Table 3: Thermal profiling of the glass temperature of the collector

System	Above-Glass Peak Temperature (°C)	Below-Glass Peak Temperature (°C)	Average Gradient Temperature (°C)
Pebble	53.5	64	10.5
Bottle Cap	67	82.5	15.5
Grit	67.5	89.5	22
No Load	60.5	76.5	16

The temperature gradient between the upper and lower surfaces of the glazing was indicative of effective solar heat entrapment. Grit exhibited the highest thermal gradient (22 °C), peaking at 89.5 °C beneath the glazing, outperforming all other configurations. This suggests superior solar energy absorption and minimal convective losses.

On the collector surface, the maximum temperature reached 112°C in the grit configuration. In comparison, the bottle cap configuration registered the highest average collector temperature (79.74°C), indicating a rapid thermal response and improved mid-day heat transfer. Pebbles demonstrated a lower thermal response (maximum: 89°C; average: 61.79°C), indicating moderate storage and release efficiency.

The outlet air temperature followed similar trends, with bottle caps and grit configurations maintaining elevated temperatures above ambient during peak solar hours, crucial for consistent drying. Notably, bottle caps sustained the highest outlet temperature differential (+45 °C), highlighting their immediate heat transfer advantage.

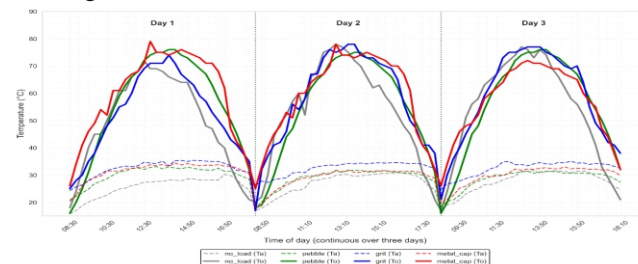


Fig. 6: Variation of ambient and outlet air temperatures over three consecutive days showing diurnal heating-cooling behaviour of different TES-integrated solar dryer configurations

Heating and cooling dynamics

Table 4: Heating and cooling dynamics of the collector in different systems

Parameter	Metal Cap (Outlet Air)	Grit Bed	Pebble Bed	No Load (Air Only)
Heating Rate (°C·h ⁻¹)	~9.85	~12.85	~16.5	~12.5
Cooling Rate (°C·h ⁻¹)	~13.6	~9.78	~10.4	~11.25
Thermal Retention	Poor	Excellent	Good	Poor
Relative charging-phase thermal efficiency	Highest	Moderate	Moderate	Low
Best Application	Quick, active drying	Extended drying	Pre-heating, buffer	Control/baseline

During the heating phase (9:00-11:00 AM), the pebble bed achieved the fastest temperature rise (~16.5 °C · h⁻¹), which is ideal for early moisture removal. However, during the cooling phase (3:00-6:00 PM), grit demonstrated superior thermal inertia (~9.78°C·h⁻¹), indicating its suitability for extended drying operations.

Heat recovery behaviour during charging and discharging phases

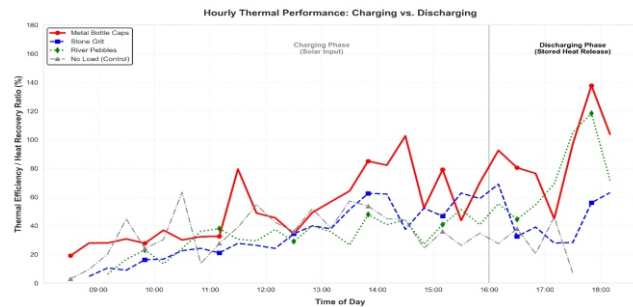


Fig. 7: Hourly variation of thermal efficiency (charging phase) and heat recovery behaviour (discharging phase) of different TES-based dryers

Table 5: Tabular chart for thermal character of different media

Configuration	Average thermal efficiency during charging phase (%)	Peak heat recovery ratio during discharging phase (%)	Time of peak
No Load	34.88	92.46	5:00–5:30 PM
Pebbles	42.26	134.20	5:30–6:00 PM
Grit	36.32	107.70	3:00–3:30 PM
Metal Bottle Caps	59.70	161.24	2:00–2:30 PM

Figure 7 presents the temporal variation of the thermal performance of the indirect passive solar dryer for different thermal energy storage (TES) configurations, highlighting distinct behaviours during the charging (sunshine) and discharging (post-sunshine) phases. The system's thermal response was strongly influenced by the presence and type of TES material, due to differences in heat absorption, retention, and release.

During the charging phase, corresponding to periods of active solar irradiance, all configurations exhibited conventional collector behaviour with thermal efficiency values remaining below unity. The average thermal efficiency during the charging phase, calculated as the mean of instantaneous efficiency values obtained only during sunshine hours, was found to be 59.70% for the metal bottle cap configuration, followed by 42.26% for pebbles, 36.32% for grit, and 34.88% for the no-load system. The superior charging-phase performance of the metal bottle caps is attributed to their higher effective heat transfer area and enhanced thermal conductivity, which promoted efficient heat absorption and storage within the collector.

As solar irradiance declined during the late afternoon, the system transitioned into the discharging phase, where the contribution of stored thermal energy became the dominant factor. In this phase, system performance was evaluated using the heat recovery ratio (HRR) rather than thermal efficiency, as the useful heat supplied to the drying air originated primarily from previously stored sensible heat. The metal bottle cap configuration demonstrated the highest peak HRR of 161.24%, occurring between 2:00–2:30 PM, followed by the pebble (134.20%) and grit (107.70%) configurations. These elevated HRR values indicate effective release of stored thermal energy and do not represent energy conversion efficiency.

In contrast, the no-load configuration exhibited limited heat recovery during the discharging phase, with a maximum HRR of 92.46%, due to the absence of thermal mass within the collector. The rapid decline in its thermal output after peak sunshine hours highlights the system's susceptibility to convective and radiative heat losses when no storage medium is present.

Overall, the results clearly demonstrate that the integration of TES significantly enhances the thermal stability and post-sunshine performance of the indirect passive solar dryer. Among the tested materials, metal bottle caps exhibited the most effective combination of high charging-phase efficiency and superior heat recovery behaviour, enabling extended drying operation during periods of reduced or absent solar radiation. Similar improvements in evening-hour drying performance through thermal mass integration have been reported in previous solar dryer studies, supporting the findings of the present work.

Operational implications and material suitability

The observed thermal behaviours provide a clear guide for

material selection. The bottle cap configuration, with its rapid thermal response and high conductivity, is ideal for high-moisture crops where immediate moisture removal is critical to stop spoilage. For crops requiring longer, steadier drying, grit is the superior choice; its high thermal inertia and slow cooling rate ($9.78^{\circ}\text{C}\cdot\text{h}^{-1}$) sustain the process effectively after sunset. Pebbles serve as a practical, low-cost alternative, despite a fast initial heat-up ($16.5^{\circ}\text{C}\cdot\text{h}^{-1}$); their lower overall charging-phase thermal efficiency (42.26%) makes them suitable for general applications where budget outweighs precision. Essentially, the choice of TES material shouldn't be arbitrary, but rather matched to the crop's specific need for either speed (such as metal bottle caps) or duration (such as grit).

Drying behaviour and kinetics

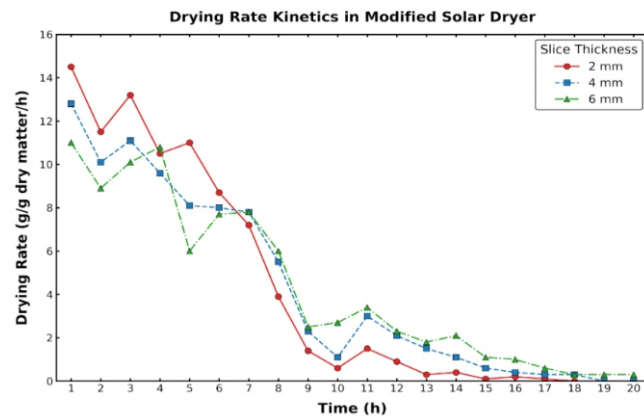


Fig. 8: Drying rate curve of modified dryer

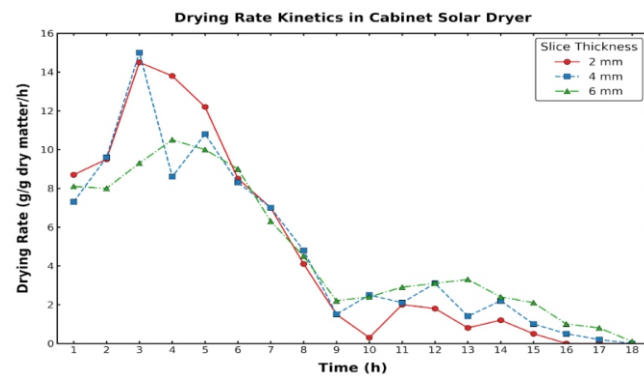


Fig. 9: Drying rate curve of cabinet dryer.

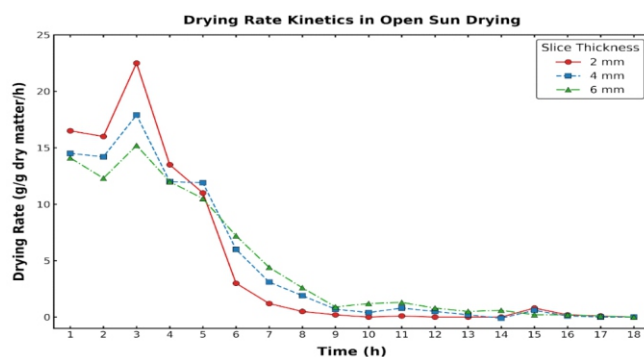


Fig. 10: Drying rate curve of open sun drying

The drying kinetics of beetroot slices were analysed across three systems: Modified Solar Dryer (MD), Cabinet Dryer (CD), and Open Sun Drying (OSD), for varying thicknesses (2, 4, and 6 mm). The drying profiles for all configurations consistently revealed a characteristic falling rate period, typical of high-moisture agricultural products, though performance characteristics varied significantly between systems.

Open Sun Drying (OSD) exhibited the highest initial drying rate, particularly for 2 mm slices (~22.5 g/g dry matter/hour). However, as shown in Figure 10, the process was highly erratic. The 4 mm slices (~17.88 g/g/hour) displayed irregular patterns, including instances of negative rates during later stages. This instability is attributed to uncontrolled environmental fluctuations and moisture reabsorption, rendering the method unsuitable for precision drying despite its initial speed.

In contrast, the Cabinet Dryer (CD) demonstrated a moderate and gradual decline in drying rates (Figure 9). While effective for thin slices—achieving a rate of ~13.61 g/g/hour for 2 mm samples and the lowest final moisture content (3.58%) due to forced convection—its performance became non-linear for thicker samples. The drying rate was variable at 4 mm (~15.02 g/g/hour) and slowed significantly for 6 mm slices (~9.29–10.53 g/g/hour), indicating limited thermal penetration and inconsistent airflow as the slice thickness increased.

The modified solar dryer (MD) emerged as the most efficient and reliable system, characterised by smooth, linear drying kinetics (Figure 8). It maintained consistent rates across all thicknesses: ~14.52 g/g/hour for 2 mm, ~12.85 g/g/hour for 4 mm, and a sustained ~11.03 g/g/hour for 6 mm slices. This superior consistency is attributed to the integrated metal bottle caps, which act as a thermal energy storage (TES) system, facilitating uniform heat distribution and minimising rate variability. Consequently, the modified dryer struck a favourable balance between drying rate and stability, making it the most suitable configuration for producing high-quality dried beetroot for quality-sensitive applications. The controlled drying rate observed in the modified system is consistent with Ankush (2024), who reported that optimised solar drying kinetics significantly improve product quality parameters compared to the erratic moisture loss typical of open sun drying.

Proximate and Nutritional Quality of Dried Beetroot

The impact of drying method and slice thickness on proximate composition and nutritional retention was substantial.

Table 6: Proximate analysis of beetroot

Parameter	T2D	T4D	T6D	T2C	T4C	T6C	T2O	T4O	T6O
Moisture (%)	5.59	5.79	6.82	3.58	4.14	5.73	6.01	6.64	7.13
Protein (%)	10.06	10.17	9.77	9.65	8.74	9.15	7.63	10.05	8.18
Fat (%)	1.6	1.29	0.73	1.26	1.2	1.07	1.97	1.63	1.37
Crude Fibre (%)	3.19	7.51	5.75	6.01	6.67	6.1	7.23	6.55	7.14
Ash (%)	5.27	5.94	6.45	6.24	5.94	5.64	5.11	5.69	6.7
Carbohydrate (%)	77.48	76.81	76.23	79.27	79.98	78.41	79.28	75.99	76.62
Ascorbic Acid (mg)	10.23	9.2	8.4	8.2	7.2	6.4	6.16	5.36	4.6
Total Phenol (mg)	119	128	104	105	129	108	105	128	106
Betalains (mg)	35.24	38.3	37.85	34.87	50.09	35.36	49.83	51.93	36.89
Betaxanthin (mg)	12.69	13.8	13.72	13.45	16.06	12.9	24.09	15.43	13.64
Betacyanin (mg)	25.54	24.5	24.13	21.42	34.03	22.46	25.74	36.5	23.25
TTA (%)	0.67	0.9	0.64	1.1	0.93	0.84	0.7	0.71	0.64

Table 7: Comprehensive review of the proximate analysis of all dryers

Colour									
L*	28.72	25.41	21.69	27.61	24.05	24.12	27.19	24.26	29.94
a*	26.88	21.27	18.82	25.93	23.25	21.52	22.87	25.26	20.36
b*	3.66	3.22	2.54	5.71	3.93	4.5	3.71	3.8	4.42

The impact of drying method and slice thickness on the macronutrient profile of beetroot was substantial. The final moisture content, a critical determinant of stability, was lowest in T2C (3.58%) and T4C (4.14%), indicating the superior efficiency of the cabinet dryer due to forced convection. In contrast, open sun drying (T6O) retained the highest moisture (7.13%), while the modified dryer achieved a favourable balance suitable for long-term storage (5.59–5.79% in T2D/T4D), aligning with optimised solar drying levels reported by Ojeniran et al. (2025). Protein retention peaked in the modified dryer (10.17% in T4D), likely due to reduced exposure to harsh temperatures compared with open-sun drying (7.63% in T2O). These results are supported by Singh et al. (2024), who found that the stable thermal environment of the TES-integrated dryer is conducive to preserving protein integrity. Fat content was highest in T2O (1.97%) and lowest in T6D (0.73%), confirming that high-heat conditions and thicker slices accelerate degradation, a trend consistent with findings by Nwaigwe et al. (2018) and Sharma et al. (2022). Regarding structural carbohydrates, crude fibre was highest in medium slices (7.51% in T4D), whereas ash content increased with slice thickness, peaking in T6O (6.70%) due to the higher mineral concentration during slower drying. Carbohydrate retention followed similar patterns, with controlled drying systems maintaining higher levels (75–82%) than open-sun drying, likely due to reduced starch hydrolysis during prolonged

exposure.

The evaluation of bioactive compounds highlighted the sensitivity of antioxidants to thermal stress. Ascorbic acid was best retained in the modified dryer (10.23 mg in T2D), significantly outperforming open sun drying (4.60 mg in T6O). The total phenolic content peaked in medium slices under both cabinet and open sun conditions (~129 mg in T4C/T4O). This suggests that a moderate slice thickness of 4 mm offers an optimal balance for antioxidant retention, matching trends reported by Ojeniran et al. (2025) and Nwaigwe et al. (2018). Pigment analysis revealed that while open sun drying preserved the highest betalains (51.93 mg in T4O) due to lower thermal stress, the modified dryer still retained appreciable levels (~38 mg in T4D) with reduced degradation compared to cabinet drying. Although open sun drying favours pigment retention, it compromises microbial safety; thus, the modified dryer offers a superior compromise for maintaining visual quality and hygiene, supporting the conclusions of Ojeniran et al. (2025) regarding the efficacy of indirect solar drying.

Physicochemical properties, specifically titratable acidity (TTA) and colour, further differentiated the drying systems. TTA ranged from 0.64% to 1.10%, with higher acidity in cabinet-dried samples suggesting a concentration effect from rapid water removal. In contrast, the modified dryer

maintained moderate temperatures that preserved the product's taste. Colour profiling (CIELAB) indicated that open sun drying caused significant surface bleaching, resulting in the highest lightness (L^*) values (29.94 in T6O), whereas the modified dryer best preserved the natural redness (a^*) of the beetroot (26.88 in T2D). Conversely, yellowness (b^*) was highest in cabinet drying, indicative of pigment rearrangement under higher heat. These trends align with established literature, which consistently shows that controlled drying preserves the characteristic redness of beetroot better than the bleaching effects of direct solar radiation (Ojeniran *et al.*, 2025; Sharma *et al.*, 2022).

Table 8: Summary of optimal drying conditions for quality retention in beetroot slices

Parameter	Observed value	Optimal configuration
Lowest Moisture	3.58%	T2C (Cabinet, 2 mm)
Highest Protein	10.17%	T4D (Modified, 4 mm)
Highest Ascorbic Acid	10.23 mg/100 g	T2D (Modified, 2 mm)
Highest Phenol	129 mg GAE/100 g	T4C (Cabinet, 4 mm)
Best Pigment Retention	51.93 mg betalains	T4O (Open Sun, 4 mm)
Best Red Colour (a^*)	26.88	T2D (Modified, 2 mm)
Highest Carbohydrate	79.98%	T4C (Cabinet, 4 mm)

Comparative Performance of Drying Systems

A comprehensive comparison of the Modified Indirect Passive Solar Dryer (IPSD), Cabinet Dryer, and Open Sun Drying reveals distinct operational characteristics in terms of thermal efficiency, moisture removal, and drying kinetics (Table 9).

Thermal efficiency

The thermal efficiency analysis highlights the superiority of the modified IPSD integrated with metal bottle caps. This configuration achieved the highest average thermal efficiency during the charging phase (59.70%) and a peak heat recovery ratio of 161.24% during the discharging phase, indicating effective utilisation of stored thermal energy. This high efficiency is attributed to the low thermal mass and high conductivity of the metal bottle caps, which facilitated rapid heat transfer to the drying air. In contrast, open sun drying relies solely on direct solar incidence with zero thermal regulation, resulting in substantial energy losses to the ambient environment. While the cabinet dryer utilises the greenhouse effect for heat generation, it lacks the active thermal storage component found in the modified IPSD, which limits its efficiency during fluctuating solar intensity.

Moisture loss and final moisture content

The cabinet dryer demonstrated the most aggressive moisture removal, achieving the lowest final moisture content of 3.58%

for 2 mm slices, compared to 5.59% for the Modified IPSD and 6.01% for Open Sun Drying. While the cabinet dryer effectively minimised moisture, the modified IPSD also successfully reduced moisture content to safe storage levels (<6%) for both 2 mm and 4 mm slices. Conversely, open sun drying failed to achieve comparable dryness for thicker slices (6 mm), retaining a high final moisture content of 7.13%, which poses a risk for microbial stability.

Drying time and kinetics

In terms of drying kinetics, open sun drying exhibited the highest initial drying rate (~22.5 g/g/h for 2 mm slices) due to unrestricted exposure to solar radiation and ambient airflow. However, this method proved highly erratic, with drying rates dropping sharply or becoming negative due to environmental fluctuations and moisture reabsorption. The Modified IPSD provided the most consistent drying profile, maintaining a stable drying rate (~12.85 g/g/h for 4 mm slices) and extending the drying process into the late afternoon due to the thermal inertia of the TES materials. This consistency prevented the case-hardening often associated with the rapid, uncontrolled drying observed in the other methods.

Table 9: Comparative summary of efficiency, moisture loss, and drying behaviour

Parameter	Modified IPSD (Metal bottle caps)	Cabinet Dryer	Open Sun Drying
Avg. Thermal Efficiency	59.70% (Highest)	N/A (Direct Gain)	N/A (Open System)
Final Moisture (2 mm)	5.59% (Safe)	3.58% (Lowest)	6.01%
Final Moisture (6 mm)	6.82%	5.73%	7.13% (Highest)
D r y i n g Behaviour	Consistent, Linear, Controlled	Rapid but Variable	Erratic, Uncontrolled
Heat Retention (Post-Sunset)	High (TES Effect)	Low	None

CONCLUSION

This study demonstrated the novel application of discarded black-painted metal bottle caps as a high-performance, zero-cost thermal energy storage (TES) medium in an indirect passive solar dryer (IPSD) for beetroot dehydration. Among the three TES materials evaluated, metal bottle caps achieved the highest average charging-phase thermal efficiency (59.70%) and a peak heat recovery ratio of 161.24% during the discharging phase, significantly outperforming pebbles (42.26%) and grit (36.32%). The high thermal conductivity of metal bottle caps enabled rapid heat transfer, sustaining outlet air temperatures up to 45°C above ambient and ensuring stable drying conditions throughout the day.

A clear trade-off between heating rate and heat retention was observed among the TES materials. Pebbles exhibited the fastest initial heating rate ($16.5^{\circ}\text{C}\cdot\text{h}^{-1}$), making them suitable for quick thermal response, whereas grit demonstrated superior thermal inertia with the slowest cooling rate ($9.78^{\circ}\text{C}\cdot\text{h}^{-1}$), favouring extended post-sunset drying. Metal bottle caps offered the best overall balance of rapid heat absorption and effective heat recovery.

Drying kinetics revealed that the modified IPSD produced the most consistent and stable drying profile across all slice thicknesses (2, 4, and 6 mm), with drying rates ranging from 11.03 to 14.52 g/g dry matter/h. In contrast, open sun drying was highly erratic despite a high initial rate, and the cabinet dryer showed inconsistent performance for thicker slices. The modified IPSD successfully reduced moisture content to safe storage levels (5.59% for 2 mm slices), preventing case-hardening and ensuring uniform dehydration.

Nutritional analysis confirmed that the modified IPSD best preserved the bioactive quality of dried beetroot. Protein retention was highest in the modified dryer (10.17% for 4 mm slices), along with superior retention of ascorbic acid (10.23 mg/100 g) and total phenolic content (128 mg/100 g) compared to open sun drying. The controlled thermal environment also preserved the natural red colour of beetroot, as indicated by the highest a^* value (26.88) among all drying methods. A slice thickness of 4 mm provided the optimal balance between drying efficiency and nutritional quality retention.

The study establishes recycled metal bottle caps as an efficient, sustainable, and economically viable TES material for passive solar drying of agricultural produce. This waste-to-resource approach bridges the gap between thermal energy storage, food security, and waste valorisation, offering a scalable solution for smallholder farmers in semi-arid regions. Future research should explore the long-term durability of metal bottle caps under repeated thermal cycling and extend the application to other high-moisture agricultural commodities.

ACKNOWLEDGEMENTS

I am grateful to Renewable Energy Engineering, College of Agricultural Engineering, Anand Agricultural University, Godhra, for providing research facilities and to the technical staff for their assistance

REFERENCES

Allouhi A. 2023. Latent thermal energy storage for solar industrial drying applications. *Sustainability* 15(17):13254. <https://doi.org/10.3390/su151713254>

Anand Inamdar V, Bagi J S and Prabbhu A. 2021. Design and development of prototype solar dryer using thermal

energy storage material for drying fruits and vegetables cultivated in Western Maharashtra. *International Research Journal of Engineering and Technology* 8:115–120.

- Ankush S. 2024. Solar drying of beetroot slices and its quality evaluation. *International Journal of Food and Fermentation Technology* 14(1):1–10. <https://doi.org/10.30954/2277-9396.01.2024.2>
- AOAC. 2005. Official methods of analysis of AOAC International (18th ed.). AOAC International.
- Bala B K and Woods J L. 1994. Simulation of the indirect natural convection solar drying of rough rice. *Solar Energy* 53(3):259–266. [https://doi.org/10.1016/0038-092X\(94\)90632-7](https://doi.org/10.1016/0038-092X(94)90632-7)
- Bhavani U, Mokenapalli S and Vellanki B. 2022. Comparative studies and quality evaluation of beetroot powder by different drying methods. *International Journal of Creative Research Thoughts* 10(4):562–570.
- Boukar M, Tchhoffo Houdji E, Tchuindjang Kwatchie D V, Tchaya G B and Raidandi D. 2024. Physical characterization of solar thermal energy storage (TES) materials for solar dryers: Case of volcanic stone (Pozzolan) in Chad. *Journal of Energy and Power Technology* 6(3): 1–18. <https://doi.org/10.21926/jept.2403014>
- Deepak C N and Behura A K. 2025. Thermal and environmental analysis of Cucumis sativus drying in a mixed mode solar dryer with combined sensible and latent heat energy storage. *Scientific Reports* 15(1): 9197. <https://doi.org/10.1038/s41598-025-91971-4>
- Ekechukwu O V and Norton B. 1997a. Review of solar-energy drying systems II: An overview of solar drying technology. *Energy Conversion and Management* 38(6): 615–655. [https://doi.org/10.1016/S0196-8904\(96\)00075-6](https://doi.org/10.1016/S0196-8904(96)00075-6)
- Ekechukwu O V and Norton B. 1997b. Review of solar-energy drying systems III: Low temperature air-heating solar collectors for crop drying applications. *Energy Conversion and Management* 38(6):657–677. [https://doi.org/10.1016/S0196-8904\(96\)00076-8](https://doi.org/10.1016/S0196-8904(96)00076-8)
- Fernandes L and Tavares P B. 2024. A review on solar drying devices: Heat transfer, air movement and type of chambers. *Solar* 4(1): 15–42. <https://doi.org/10.3390/solar4010002>
- Food Safety and Standards Authority of India (FSSAI). 2016. Manual of methods of analysis of foods: Food safety and standards. Ministry of Health and Family Welfare, Government of India.
- Fudholi A, Sopian K, Ruslan M H, Alghoul M A and Sulaiman M Y. 2010. Review of solar dryers for agricultural and marine products. *Renewable and Sustainable Energy Reviews* 14(1): 1–30. <https://doi.org/10.1016/j.rser.2009.07.032>

- Gupta P M, Das A S, Barai R C, Pusadkar S C and Pawar V G. 2017. Design and construction of solar dryer for drying agricultural products. *International Research Journal of Engineering and Technology* 4(6):2542–2545.
- Kalidasan B, Pandey A K, Shahabuddin S, Samykano M, Thirugnanasambandam M and Saidur R. 2020. Phase change materials integrated solar thermal energy systems: Global trends and current practices in experimental approaches. *Journal of Energy Storage* 27: 101118. <https://doi.org/10.1016/j.est.2019.101118>
- Kapadiya S and Desai M A. 2014. Solar drying of natural and food products: A review. *International Journal of Agriculture and Food Science Technology* 5(6): 459–466.
- Koçak B, Fernandez A I and Paksoy H. 2020. Review on sensible thermal energy storage for industrial solar applications and sustainability aspects. *Solar Energy* 209: 113–169. <https://doi.org/10.1016/j.solener.2020.08.081>
- Kumar B, Kumar V and Singh H K. 2015. Analysis of thermal performance of solar air dryer for three different absorber plates. *International Journal of Science, Engineering and Technology* 3(4):1087–1092. <https://doi.org/10.2348/IJSET07151087>
- Malik C P and Singh M B. 1980. Plant enzymology and histoenzymology. Kalyani Publishers.
- Matavel C, Kächele H, Steinke J, Rybak C, Hoffmann H, Salavessa J, Sieber S and Müller K. 2022. Effect of passive solar drying on food security in rural Mozambique. *Scientific Reports* 12(1): 19302. <https://doi.org/10.1038/s41598-022-22129-9>
- Mehta P, Patel V, Kumar S, Sharma V, Tejani G G and Santhosh A J. 2025. Performance assessment of thermal energy storage system for solar thermal applications. *Scientific Reports* 15(1): 92458. <https://doi.org/10.1038/s41598-025-92458-y>
- Nwagwe K N, Okoronkwo C A and Onyeka E U. 2018. Effect of different drying methods on red beet (*Beta vulgaris*) quality. *Scientia Ricerca: Nutrition and Food Technology* 2(1): 65–72. <https://scientiaricerca.com/srnuft/SRNUFT-02-00065.php>
- Ojeniran J I, Adejumo B A and Obasa P A. 2025. Effects of drying methods on the qualities of beetroot flour. *European Journal of Sustainable Development Research* 9(3): em0312. <https://doi.org/10.29333/ejosdr/16357>
- Onuigbo F I, Abdulrahman S and Ayodeji A E. 2017. Construction of a direct solar dryer for perishable farm products. *International Journal of Scientific Research Engineering & Technology* 6(2):1–5. <https://doi.org/10.13140/RG.2.2.31220.68482>
- Ranganna S. 1986. Handbook of analysis and quality control for fruit and vegetable products (2nd ed.). McGraw Hill Education.
- Rulazi E L, Marwa J, Kichonge B and Kivevele T. 2023. Development and performance evaluation of a novel solar dryer integrated with thermal energy storage system for drying of agricultural products. *ACS Omega* 8(45): 43304–43317. <https://doi.org/10.1021/acsomega.3c07314>
- Shakir B K and Simone V. 2024. Estimation of betalain content in beetroot peel powder. *Italian Journal of Food Science* 36(1): 53–57. <https://doi.org/10.15586/IJFS.V36I1.2438>
- Sharma G P, Prasad S and Chahar V K. 2022. Effect of drying methods on colour kinetics and quality characteristics of beetroot (*Beta vulgaris* L.) slices. *Journal of Food Science and Technology* 59(8): 3233–3242. <https://doi.org/10.1007/s13197-022-05456-1>
- Singh P, Khanna S, Srivastav S and Chauhan E S. 2024. Nutritional analysis of beetroot (*Beta vulgaris* L.) and its potential in development of value-added food product. *Asian Journal of Basic Science & Research* 6(4): 42–48. <https://doi.org/10.38177/AJBSR.2024.6404>
- Singleton V L and Rossi J A. 1965. Colorimetry of total phenolics with phosphomolybdic-phosphotungstic acid reagents. *American Journal of Enology and Viticulture* 16(3):144–158.

Citation:

Kumar A, Vyas D K and Jogunuri S. 2026. Nutritional evaluation of beetroot dried using novel thermal storage-based passive solar dryers. *Journal of AgriSearch* 13(1): 43-53.